Model-based Robust Fault Diagnosis for Satellite Control Systems Using Learning and Sliding Mode Approaches

Qing Wu, Mehrdad Saif
School of Engineering Science, Simon Fraser University, Vancouver, BC, Canada
Email: {qingw, saif}@ensc.sfu.ca

Abstract— **In this paper, our recent work on robust model-based fault diagnosis (FD) for several satellite control systems using learning and sliding mode approaches are summarized. Firstly, a variety of nonlinear mathematical models for these satellite control systems are described and analyzed for the purpose of fault diagnosis. These satellite control systems are classified into two classes of nonlinear dynamical systems. Then, several fault diagnostic observers using sliding mode and learning approaches are presented. Sliding mode with time-varying switching gains, second order sliding mode, and high order sliding mode differentiators are respectively used in the proposed diagnostic observers to deal with modeling uncertainties. Neural model-based and iterative learning algorithms-based online learning estimators are respectively used in the diagnostic observers for the purpose of isolating and estimating faults. Finally, conclusions and future work on the health monitoring and fault diagnosis for satellite control systems are provided.**

Index Terms— **fault diagnosis, observer, sliding mode, learning, satellite control systems**

I. INTRODUCTION

With the development of space technologies, different classes of satellites have been constructed and utilized for various space missions, such as global positioning, Earth observation, atmosphere data collection, space science, and communication. The dynamics of satellite control systems have the following characteristics: i) The safety and reliability of the satellite control systems are so essential that fault diagnosis (FD) strategies are indispensable for them. ii) Various linear and nonlinear mathematical models of the satellite control systems are available for the design and analysis of controllers and/or state observers. Although linear models can represent the attitude dynamics at local vertical local horizontal (LVLH) orientation, inherently, the satellite dynamics is nonlinear. Especially when a satellite make a large angle maneuver, or it has flexible appendages, or multiple satellites are deployed, different nonlinear models must be applied to describe these dynamics. iii) The satellites in space are subject to internal modeling uncertainties and external disturbances, such as gravity-gradient torque, aerodynamics torque, and Earth magnetic torque, etc. iv) In order to ensure the normal operation, real-time fault diagnosis is necessary to provide information for the satellites to accommodate the fault in time.

In the last three decades, model-based robust fault diagnosis schemes for nonlinear dynamic systems have been significantly investigated. Many contributions have been summarized in the books [3] and [4]. For nonlinear systems, a class of FD schemes using learning methodologies, which use neural networks [5], [6], [7], iterative learning observers, [8], or adaptive observers [9], [10], [11], have received great deal of attention. To achieve robust fault diagnosis, dead-zone operators are adopted in the learning methodologies to make the fault approximator insensitive to the error signal under a certain threshold which is considered to be caused by modeling uncertainties [12], [13], [14]. However, two issues in this class of methodologies still need further studies. One is that, in all likelihood, the dead-zone operators may reduce the accuracy of the fault approximation. The other issue is that the projection operators, which can confine the parameter estimation vectors to a predefined compact and convex region, have to be used to bound parameters in the presence of modeling uncertainties and approximation errors.

Moreover, due to the inherent robustness to system uncertainties, traditional and high order sliding mode have been studied in system observation (e.g. [15], [16], [17], [18], [20], [21], [22]) and robust fault diagnosis (e.g. [23], [24], [25], [26]), [27] for many years. One FD method based on sliding mode is that the estimation dynamics maintain a sliding motion even in the presence of fault, and the fault is reconstructed by manipulating the equivalent output injection signal. Another approach is to design an observer in such a way that the sliding motion is destroyed in the presence of fault [28]. In this case, additional online estimators are needed to approximate the fault.

In this paper, we summarize our recent study on the robust fault diagnosis for a variety of satellite control systems using sliding mode and learning approaches. Our objective is to take advantages of these two methodologies and create novel and practical model-based robust fault diagnosis schemes for various satellite control systems. In Section II, the satellite control systems in our study

This paper is based on "An Overview of Robust Model-based Fault Diagnosis for Satellite Systems Using Sliding Mode and Learning Approaches," by Q. Wu and M. Saif, which appeared in the Proceedings of the IEEE Conference on Systems, Men, and Cybernetics, Montreal, Canada, October, 2007. © 2007 IEEE.

are presented and summarized. Then, these systems are described by two families of mathematical formula in Section III. After that, Section IV proposes three kinds of observers using sliding mode and learning approaches. Fault detection, isolation, and estimation schemes based on these diagnostic observers are formulated in Section V and VI. Finally, conclusion is given in Section VII.

II. SATELLITE MODELS

In mathematical model-based fault diagnosis schemes, a model for the plant is built first. Then diagnostic residuals are generate through comparing the output of the practical system with the output of the model. Next, the residuals are used to diagnose faults.

An important assumption for the model-based fault diagnosis schemes is that the mathematical models are able to represent the practical systems with sufficient accuracy. Otherwise, the mismatch between the practical systems and their models as well as disturbances might cause the proposed fault diagnosis schemes unreliable. As aerospace technologies develop, different models for satellites are available for system analysis and controller design. The satellite models become more and more sophisticated if they are used to represent the real satellite systems precisely. Hence, more complex models should also be used in the model-based robust FD for satellite control systems.

A. Nonlinear Model for Rigid-body Satellite Attitude Control Systems

In many research literatures, a satellite is modeled as a rotary rigid body, and its dynamics is described using the following equation of motion [29],

$$I\dot{\omega} + \omega^{\times} I\omega = 3\omega_0^2 \zeta^{\times} I\zeta + u + T_d \tag{1}$$

and the following relation between ω and pitch angle θ_1, yaw angle θ_2, and roll angle θ_3:

$$\begin{aligned}\omega = \begin{bmatrix}\omega_1\\ \omega_2\\ \omega_3\end{bmatrix} &= \begin{bmatrix}(\omega_0+\dot{\theta}_1)\sin\theta_2 + \dot{\theta}_3\\ (\omega_0+\dot{\theta}_1)\cos\theta_2\cos\theta_3 + \dot{\theta}_2\sin\theta_3\\ -(\omega_0+\dot{\theta}_1)\cos\theta_2\sin\theta_3 + \dot{\theta}_2\cos\theta_3\end{bmatrix}\\ &= \begin{bmatrix}\sin\theta_2 & 0 & 1\\ \cos\theta_2\cos\theta_3 & \sin\theta_3 & 0\\ -\cos\theta_2\sin\theta_3 & \cos\theta_3 & 0\end{bmatrix}\begin{bmatrix}\dot{\theta}_1\\ \dot{\theta}_2\\ \dot{\theta}_3\end{bmatrix}\\ &\quad + \begin{bmatrix}\omega_0\sin\theta_2\\ \omega_0\cos\theta_2\cos\theta_3\\ -\omega_0\cos\theta_2\sin\theta_3\end{bmatrix}\\ &= R(\theta)\dot{\theta} + \omega_c(\theta)\end{aligned} \tag{2}$$

where ω_0 is the orbital angular velocity of the satellite, $\theta = [\theta_1\ \theta_2\ \theta_3]^{\top}$ is Euler angle vector, $u = [u_1, u_2, u_3]^{\top}$ is the control torque vector, and T_d represents the external disturbance torques. $I_i, (i = 1, 2, 3)$ are the principal axis moments of inertia of the satellite. The term ζ is

$$\zeta = \begin{bmatrix}-\sin\theta_1\cos\theta_2\\ \cos\theta_1\sin\theta_3 + \sin\theta_1\sin\theta_2\cos\theta_3\\ \cos\theta_1\cos\theta_3 - \sin\theta_1\sin\theta_2\sin\theta_3\end{bmatrix} \tag{3}$$

The notation $\omega^{\times}$ stands for a skew symmetric matrix

$$\omega^{\times} = \begin{bmatrix}0 & -\omega_3 & \omega_2\\ \omega_3 & 0 & -\omega_1\\ -\omega_2 & \omega_1 & 0\end{bmatrix}$$

For the dynamic system represented by (1) and (2), only θ_1, θ_2, θ_3 are measurable.

B. Linear Model for Rigid-body Satellite Attitude Systems

For small attitude deviation from LVLH orientation, the nonlinear dynamics of the satellite attitude control systems can be linearized around its equilibrium point, and a linear model is given in [30] as

$$\begin{aligned}&I_1\ddot{\theta}_3 - w_0(I_1 - I_2 + I_3)\dot{\theta}_2 + 4w_0(I_2 - I_3)\theta_1 = u_1 + T_{d1}\\ &I_2\ddot{\theta}_1 + 3w_0^2(I_1 - I_3)\theta_1 = u_2 + T_{d2}\\ &I_3\ddot{\theta}_2 + w_0(I_1 - I_2 + I_3)\dot{\theta}_3 + w_0^2(I_2 - I_1)\theta_2 = u_3 + T_{d3}\end{aligned} \tag{4}$$

This linear model is important, since it can represent a class of micro-satellites that have wide applications. Many control algorithms can be designed based on this linear model. Moreover, for this linear time invariant systems, fault diagnosis based on linear models can be completely solved, provided the considered system is observable.

C. Quaternion-based Model for Satellite Attitude Systems

Quaternions were invented as a result of searching for hypercomplex numbers that could be represented by points in three dimensional space. Quaternions have no inherent geometric singularity as do Euler angles. Moreover, quaternions are well suitable for onboard real-time computation because only products and no trigonometric relations exist in the quaternion kinematic differential equations. Thus, spacecraft orientation is now commonly represented in terms of quaternions. The motion equations of the satellite are described in [31] as

$$I\dot{\omega} = -S(\omega)I\omega + T_d + u \tag{5}$$

$$\dot{q} = \frac{1}{2}(q_4 I + S(q)) \tag{6}$$

$$\dot{q}_4 = -\frac{1}{2}q^{\top}\omega \tag{7}$$

where I is still the moment of inertia matrix, ω is the angular velocity of the satellite, T_d denotes the disturbance torque, u is also the control torque, $q = [q_1, q_2, q_3]^{\top}$, and q_4 constitute the quaternions of the satellite, which satisfy $q^{\top}q + q_4^2 = 1$. The quaternions are the output of the system (5)-(7). The notation $S(\omega)$ is the skew symmetric matrix.

D. Model for Flexible Satellite Attitude Systems

As the second generation of satellites appear, flexible satellites have been deployed. The model of a flexible satellite consists of a rigid central hub, which represents the satellite body, and two flexible appendages, which are usually solar arrays, antennas, or any other flexible structures.

Spatial discretization method has ever been used to derive a group of ordinary differential equations to describe the motion of satellite, although the vibration of the appendages is formulated by partial differential equations. Hence, the appendage deflections are expressed in terms of a set of admissible or shape functions as

$$\delta(l,t) = \sum_{i=1}^{N} \Psi_i(l-r)p_i(t) \tag{8}$$

where $p_i(t)$ are the generalized coordinates associated with these functions, l is the distance from a point on the appendage to the center of the hub, and r is the radius of the hub. Here, we assume that N modes are sufficient for the computation of elastic deformation. Ψ_i are the shape functions that satisfy the geometric and physical boundary conditions. The shape functions are given in [32] that

$$\Psi_i(l-r) = 1 - \cos\left(\frac{i\pi(l-r)}{L}\right) + \frac{1}{2}(-1)^{i+1}\left(\frac{i\pi(l-r)}{L}\right)^2 \tag{9}$$

A simplified formulation of the governing equations of this class of satellites is given in [33]

$$\begin{bmatrix} J_t & \mathbf{m}_{\psi\mathbf{p}}^{\top} \\ \mathbf{m}_{\psi\mathbf{p}} & \mathbf{M_{pp}} \end{bmatrix}\begin{bmatrix} \ddot{\psi} \\ \ddot{\mathbf{p}} \end{bmatrix} + \begin{bmatrix} 0 & 0 \\ 0 & \mathbf{C_{pp}} \end{bmatrix}\begin{bmatrix} \dot{\psi} \\ \dot{\mathbf{p}} \end{bmatrix} + \begin{bmatrix} 0 & 0 \\ 0 & \mathbf{K_{pp}} \end{bmatrix}\begin{bmatrix} \psi \\ \mathbf{p} \end{bmatrix} = \begin{bmatrix} u_t \\ 0 \end{bmatrix} + \begin{bmatrix} h_1 \\ \mathbf{h_2} \end{bmatrix} \tag{10}$$

where

$$J_t = J + 2J_1$$
$$h_1 = -3\omega_0^2 J_1 \sin(2\psi) - 3\omega_0^2 \cos(2\psi)\mathbf{m}_{\psi\mathbf{p}}^{\top}\mathbf{p}$$
$$\mathbf{h_2} = (\dot{\psi}^2 + 2\dot{\psi}\omega_0 + 3\omega_0^2 \sin^2\psi)\mathbf{M_{pp}p} - \frac{3}{2}\omega_0^2 \sin 2\psi \mathbf{m}_{\psi\mathbf{p}}$$

where ψ is the pitch angle, $\mathbf{p} = [p_1, \cdots, p_N]^{\top}$ is the vector of appendage flexibility generalized coordinates, ω_0 is the orbital rate, J and J_1 are the mass moments of inertia of the central hub and each appendage, respectively, u_t is the control torque, and $\mathbf{M_{pp}}$, $\mathbf{m}_{\psi\mathbf{p}}$, $\mathbf{C_{pp}}$ and $\mathbf{K_{pp}}$ are the following modal integrals [33] as

$$[\mathbf{M_{pp}}]_{i,j} = 2\int_r^{r+L} \Psi_i(l-r)\Psi_j(l-r)dl$$
$$[\mathbf{m}_{\psi\mathbf{p}}]_{i,j} = 2r\int_r^{r+L} l\Psi_i(l-r)dl$$
$$[\mathbf{C_{pp}}]_{i,j} = 2\int_r^{r+L} CI\Psi_i''(l-r)\Psi_j''(l-r)dl$$
$$[\mathbf{K_{pp}}]_{i,j} = 2\int_r^{r+L} EI\Psi_i''(l-r)\Psi_j''(l-r)dl \tag{11}$$

where $\Psi_i'' = (\partial^2\Psi_i/\partial l^2)$, C and E are the damping coefficient and modulus of elasticity of the appendages, respectively, and I is the sectional area moment of inertia with respect to the appendage bending axis.

E. Model for Satellite Orbital Control Systems

The above model A, B and C are all about attitude dynamics of satellites. When we consider the orbital behavior of a satellite, it can be treated as a point mass, which flies in a plane, subject to an inverse square law force field with potential energy k/r and both radial and tangential thrusts u_1 and u_2, respectively. The orbital dynamics of a point mass satellite is given by [34]

$$\begin{aligned} \dot{r} &= v & r(0) &= r_0 \\ \dot{v} &= rw^2 - \frac{k}{mr^2} + \frac{u_1}{m} & v(0) &= 0 \\ \dot{\phi} &= w & \phi(0) &= 0 \\ \dot{\omega} &= -\frac{2v\omega}{r} + \frac{u_2}{mr} & \omega(0) &= \omega_0 \end{aligned} \tag{12}$$

where m is the mass of the satellite, (r, ϕ) are the polar coordinates of the satellite, v is the radial speed, and ω is the angular speed. The control objective is to track r and ω to their reference values.

F. Model for Multiple Satellites Formation Flying System

One key technology in aerospace engineering is to distribute functionality of a large spacecraft to a group of smaller, low-cost, cooperative spacecraft. Flying two or more satellites in a specific formation is usually referred to as multiple satellite formation flying (MSFF).

MSFF is a cluster of interdependent micro-satellites that communicate with each other and share payload, data, and missions. In the simplest case, the MSFF fleet is composed of a leader satellite and a follower satellite. The leader satellite provides the reference motion trajectory and the follower satellite navigates in the neighborhood of the leader satellite according to a desired relative trajectory.

The nonlinear position dynamics of the follower satellite relative to the coordinate frame of the leader satellite is [35]

$$m_f\ddot{q} + C\dot{q} + N + T_d = u \tag{13}$$

where $C(\omega)$ denotes the following Coriolis-like matrix:

$$C = 2m_f\omega\begin{bmatrix} 0 & -1 & 0 \\ 1 & 0 & 0 \\ 0 & 0 & 0 \end{bmatrix} \tag{14}$$

and $N(q, \omega, \rho, u_l)$ denotes the following nonlinear vector

$$N = \begin{bmatrix} m_f MG\frac{q_x}{\|\rho+q\|^3} - m_f\omega^2 q_x + \frac{m_f}{m_l}u_{lx} \\ m_f MG\left(\frac{q_y+\|\rho\|}{\|\rho+q\|^3} - \frac{1}{\|\rho\|^2}\right) - m_f\omega^2 q_y + \frac{m_f}{m_l}u_{ly} \\ m_f MG\frac{q_z}{\|\rho+q\|^3} + \frac{m_f}{m_l}u_{lz} \end{bmatrix}$$

and $T_d \in \Re^3$ is the total disturbance vector.

In (13), m_l, and m_f denote the masses of the leader and follower satellite, respectively, and $u_l(t) = [u_{lx}\, u_{ly}\, u_{lz}]$, and $u_f(t)$ denote the control input vectors of the leader and follower satellite, respectively, M is the mass of the Earth, and G represents the universal gravity constant, $\rho(t) \in \Re^3$ denotes a position vector from the origin of the inertial coordinate to the leader satellite, $q(t) = [q_x\, q_y\, q_z]^{\top}$ is the relative position vector, which is to be controlled to track the desired relative position trajectory.

G. Summary of Satellite Models

From above various satellite models, we can see that firstly, no single mathematical model can represent all classes of satellite dynamics, especially, when the satellite can not be simply described as a rigid body. Secondly, mathematical description of the investigated satellite control systems are classified and summarized. Thirdly, the main problems in controller and/or observer design for satellite systems are nonlinearity, modeling uncertainties and disturbances, which in practice are the moment-of-inertia variation and space environmental disturbances. For example, gravity-gradient torque, aerodynamic torque, and Earth magnetic torque are the primary environmental disturbances for satellite in low-Earth orbit within 1000 km [30]. Hence, nonlinearity and robustness should be carefully considered when we design fault diagnosis schemes.

Moreover, gas jet and momentum wheel are two main actuators in satellite systems. In our research, the inner mechanism of the actuator is hidden by its outside control torque. So far, we focus on robust fault diagnosis for process fault in satellite systems, which may occur in the actuator or system components of the satellite.

III. System Formulations

The above satellite control systems dynamics A-F, can be described by two families of nonlinear systems. The first class of nonlinear systems with modeling uncertainties and process faults can be described as

$$\dot{x}_1 = x_2 \tag{15}$$

$$\dot{x}_2 = f(x_1, x_2, t) + \xi(x, u, t) + \eta(x, u, t) + \mathcal{B}(t - T_f) f_a(t) \tag{16}$$

$$y(t) = x_1 \tag{17}$$

where $x_1 \in \Re^p$ and $x_2 \in \Re^p$ constitute the state vector, $u \in \Re^m$ is the control input, $y \in \Re^p$ is the output vector, respectively, $f : \Re^n \times \Re^+ \to \Re^n$, $\xi : \Re^n \times \Re^m \times \Re^+ \to \Re^n$, $\eta : \Re^n \times \Re^m \times \Re^+ \to \Re^n$, and $f_a : \Re^n \times \Re^+ \to \Re^n$ are all smooth vector fields. The nonlinear function $\eta(x, u, t)$ represents modeling uncertainties and disturbances in the system dynamics. The term $\mathcal{B}(t - T_f)$ is a time function, which is one if $t > T_f$, otherwise is zero. The nonlinear vector $f_a(t)$ denotes the changes in system dynamics due to additive state faults, which are probably caused in the actuators and/or in the system components.

Remark 1: The dynamic system (15) can represent a family of systems which have triangular input form. Satellite control systems B, D, E, and F have this structure. Many mechanical or equivalent systems can be classified into (15) because usually only displacements or angles are measurable. For such class of systems, it is possible to design an observer which does not use the input derivative. In real applications such as satellite jet control or AC motor with PWM control, the exact information of the input derivative is hard to obtained [19].

The satellite attitude control systems A and C can be described by another class of nonlinear systems, which is presented as

$$\dot{x}_1 = h(x_1, x_2) \tag{18}$$

$$\dot{x}_2 = f(x_1, x_2) + Bu(t) + \eta(t) + \mathcal{B}(t - T_f) f_a(t) \tag{19}$$

$$x_2 = h^\dagger(x_1, \dot{x}_1) \tag{20}$$

$$y = x_1 \tag{21}$$

where $x_1 \in \Re^n$, $x = [x_1^\top, x_2^\top]^\top$ is the vector of the system state, $u(t) = [u_1, \cdots, u_m]^\top$ and $y(t)$ are the system input and output vectors. Function vectors $f(x_1, x_2) = [f_1(x_1, x_2), \cdots, f_n(x_1, x_2)]^\top$ and $h(x_1, x_2) = [h_1(x_1, x_2), \cdots, h_n(x_1, x_2)]^\top$ describe the system state and output dynamics, respectively, $\eta(t) = [\eta_1(t), \cdots, \eta_n(t)]^\top$ denotes the uncertainty vector, and $f_a(t) = [f_a^{(1)}(t), \cdots, f_a^{(n)}(t)]^\top$ is the fault function vector. Moreover, $B \in \Re^{n \times m}$ is the control matrix, and, in (20), $h^\dagger$ is a pseudo-inverse function of (18), which implies the state x_2 can be described as a nonlinear function of the system output and its derivative.

For nonlinear systems, a general theory of globally convergent observers is not known yet, with the exception of some theoretical cases. We have to design *ad hoc* nonlinear observers. Moreover, the purpose of fault diagnosis does not confine to the judgment of the occurrence of fault and localization of the fault. Accurate fault information can be useful for fault tolerant purpose. Therefore, in our research, fault estimation or identification is also supposed to be realized.

IV. Diagnostic Observers

A. Diagnostic Observer Design Using Sliding Mode

In the robust fault diagnosis schemes for nonlinear systems using sliding mode observer, one method is to treat fault in the same way as uncertainties, both of which are eliminated by sliding mode [23]. In this approach, fault can be constructed through suitable matrix manipulation. Another fault diagnosis scheme using sliding mode observer is to separate the modeling uncertainties from faults in terms of their magnitude. The fault signal with magnitude above a threshold is approximated by an additional online estimator.

In order to realize fault detection, isolation, and estimation, we proposed a class of nonlinear observers, which combine sliding mode observer with various online estimators. The sliding mode observer is to achieve robust state estimation, which reduces the effect of initial state estimation error and modeling uncertainties on the state estimation. The successful state estimation provides more accurate information on the process fault, which is estimated by the online estimator.

The dynamic system (15) represents a class of systems which have triangular input form. Sliding mode observers for this class of systems have been studied [20]. In their methods, the states are stabilized one by one in a recursive way within a finite time. A constant switching gain in their sliding mode observer is acceptable because

their objective is only to observe the states. However, when there is a need to eliminate the effect of modeling uncertainties and for the sliding motion to be destroyed as a fault occurs, a time-varying sliding mode gain is preferred.

Thus, a nonlinear diagnostic observer was proposed in [37]

$$\dot{\hat{x}}_1 = \hat{x}_2 + g_1(t)\text{sign}(\Gamma_1 s_1(t)) + \mathcal{B}(t-T_e)\hat{M}_1(t) \quad (22)$$

$$\dot{\hat{x}}_2 = f(\hat{x}_1, \hat{x}_2, t) + \xi(\hat{x}, u, t) + g_2(t)\text{sign}(\Gamma_2 s_2(t)) + \mathcal{B}(t-T_e)\hat{M}_2(t) \quad (23)$$

$$\hat{y} = C\hat{x} \quad (24)$$

where $\hat{x}_1 \in \Re^p$ and $\hat{x}_2 \in \Re^p$ are the states of the observer, and $\hat{y} \in \Re^p$ is the output of the observer. The term "sign" represents signum function, and $\hat{M}_1(t)$ and $\hat{M}_2(t)$ are online estimators to specify the process fault, which will be discussed in the next section. In order to separate the roles of the sliding mode observer and the online fault estimator, we disable the estimator before all the states are stabilized by the sliding mode, and a fault is assumed to occur after the estimators are activated, i.e., $T_e < T_f$.

The terms $\Gamma_1 \in \Re^{p\times p}$ and $\Gamma_2 \in \Re^{p\times p}$ are both symmetric positive definite matrices, which are useful for the theoretical proof. The terms $s_1(t) = [s_{1,1}, \cdots, s_{1,p}]^\top \in \Re^p$, and $s_2(t) = [s_{2,1}, \cdots, s_{2,p}]^\top \in \Re^p$ are named equivalent state estimation errors, which are computed according to the anti-peaking structure as follows,

$$\begin{cases} s_1(t) = x_1(t) - \hat{x}_1(t) \\ s_2(t) = (g_1(t)\text{sign}(\Gamma_1 s_1(t)))_{eq} \\ \qquad\qquad \text{if } \tilde{x}_1(t) = 0 \text{ and } \dot{\tilde{x}}_1(t) = 0 \\ \quad = 0 \qquad \text{otherwise} \end{cases} \quad (25)$$

where the $(g_1(t)\text{sign}(\Gamma_1 s_1(t)))_{eq}$, named equivalent output injection, is the average value of the discontinuous term in sliding mode, which itself is enough to keep $\tilde{x}_1$ on the sliding manifold. The switching gain $g_1(t) = diag\{g_{1,1}, \cdots, g_{1,p}\}$ and $g_2(t) = diag\{g_{2,1}, \cdots, g_{2,p}\}$ are two diagonal matrices.

The principle of the anti-peaking structure is that the output estimation error is not used to construct the state estimation error before reaching the sliding manifold [20]. Hence, the output estimation error $\tilde{x}_1 = x_1 - \hat{x}_1$ reaches the sliding manifold prior to $\tilde{x}_2 = x_2 - \hat{x}_2$. From (25), the state estimation error $\tilde{x}_2$ is constructed by the equivalent output injection as

$$\tilde{x}_2(t) = (g_1(t)\text{sign}(\Gamma_1 \tilde{x}_1(t)))_{eq} \quad (26)$$

after $\tilde{x}_1(t)$ reaches the sliding manifold.

The equivalent output injection can be calculated by using a low pass filter [17] or replace the discontinuous signum function by a continuous function [23].

For sliding mode observers, a large switching gain would enable the state estimation errors to approach the sliding manifold more quickly, but it may also cause unnecessary high-frequency chattering. Furthermore, since the sliding mode observer in our work is used only to eliminate the effect of modeling uncertainties, the switching gain can not be too large since in that case the effect of the fault will also be destroyed by the sliding mode term. On the contrary, when a fault occurs, the sliding motion should be destroyed immediately, and then the online estimators specify the fault. Therefore, a time-varying switching gain is more desirable.

In our research, two iterative methods were used to update the switching gain of the sliding mode observer [37].

1) Iterative Learning Update Law: A *P-type* iterative learning update law was designed to update the switching gain [37] as

$$G_{j+1}(t) = G_j(t) + \Phi(t)|\bar{S}_j(t)|\text{sign}(\bar{S}_j(t)\bar{S}_{j-1}(t)) \quad (27)$$

where matrix $\bar{S} = diag\{s_{1,1}, \cdots, s_{1,p}, s_{2,1}, \cdots, s_{2,p}\}$ is composed of equivalent state estimation error, and j indicates the jth iteration at time t. $\Phi(t) \in \Re^{n\times n}$ is a positive definite iterative learning coefficient matrix which determines the rate of update. The operator $|\cdot|$ takes absolute value of each element of a vector or a matrix.

The purpose of above update law (27) is to search an optimal switching gain $G^*(t)$ at each time t, which can sufficiently minimize the state estimation error. It shows that if the state estimation error has not reached the sliding manifold (the switching gain should be larger), the element of $\text{sign}(\bar{S}_j(t)\bar{S}_{j-1}(t))$ is +1, and the switching gain will increase correspondingly. If the state estimation error crosses the sliding manifold (the switching gain should be reduced), the element of $\text{sign}(\bar{S}_j(t)\bar{S}_{j-1}(t))$ is -1, and the gain will decrease correspondingly.

In an ideal case, the optimal switching gain at each time t is obtained through iteratively updating the switching gain to drive $\bar{S}_j(t)$ to the sliding manifold. In practical computation, a maximum iteration number is used to prevent a long-time update. This maximum iteration number is set to a large value in order to ensure the convergence of the switching gain to its optimal value.

2) Iterative Fuzzy Logic Update Law: In the above iterative learning update algorithm, the constant coefficient matrix $\Phi(t)$ determines the changing speed of the switching gain. In order to obtain a better performance, we consider to use fuzzy logic to update the coefficient matrix $\Phi_{i,i}(j)$ iteratively, which is given in [37] as:

$$G_{i,i}(j+1) = G_{i,i}(j) + \Phi_{i,i}(j)|\bar{S}_{i,i}(j)| \quad (28)$$

where j still denotes iteration number, and the subscript (i,i) represents the ith diagonal element of a matrix.

According to the analysis in previous section, when tuning the switching gain, not only do we need to consider the magnitude of the estimation error, but also we need to consider its position relative to the sliding manifold. Therefore, $\Phi_{i,i}(j)$ is determined based on the values of $\bar{S}_{i,i}(j-1)$ and $\bar{S}_{i,i}(j)$.

Firstly, the inputs of the fuzzy model are defined as $\nu_1 = \bar{S}_{i,i}(j-1)$ and $\nu_2 = \bar{S}_{i,i}(j)$. Then, in fuzzification of these two inputs, we map the crisp values of $\bar{S}_{i,i}(j-1)$ and $\bar{S}_{i,i}(j)$ into several fuzzy sets: NL, NB, NM, NS, PS, PM, PB, PL, where N stands for negative, P positive,

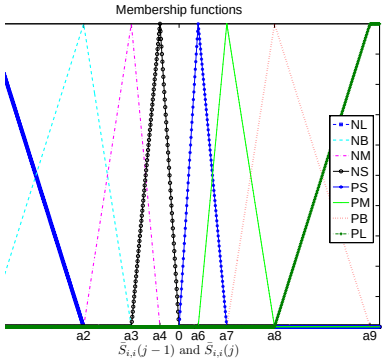

Figure 1. Membership functions for fuzzification of $\bar{S}_{i,i}(j-1)$ and $\bar{S}_{i,i}(j)$

TABLE I.
FUZZY RULE BASE FOR THE COEFFICIENT GAIN $\bar{\Phi}^n_{i,i}$

$\nu_1 \setminus \nu_2$	NL	NB	NM	NS	PS	PM	PB	PL
NL	PL	PB	PM	PS	NS	NM	NB	NL
NB	PL	PB	PM	PS	NS	NM	NB	NL
NM	PL	PB	PM	PS	NS	NM	NB	NL
NS	NL	NB	NM	NS	NS	NM	NB	NL
PS	NL	NB	NM	NS	NS	NM	NB	NL
PM	NL	NB	NM	NS	PS	PM	PB	PL
PB	NL	NB	NM	NS	PS	PM	PB	PL
PL	NL	NB	NM	NS	PS	PM	PB	PL

L large, B big, M medium, S small. The membership functions for these fuzzy sets are shown in Figure 1.

A fuzzy linguistic model (Mamdani model) is designed and shown in Table I, in which rule n is given by

$$R_n: \textbf{ If } \nu_1 \text{ is } A_{1,n} \textbf{ and } \nu_2 \text{ is } A_{2,n} \textbf{ then } \Phi_{i,i}(j) \text{ is } \bar{\Phi}^n_{i,i}$$

where R_n denotes the nth rule, $n = 1, \cdots, N_r$, and N_r is the number of rules. $A_{m,n}$ and $\bar{\Phi}^n_{i,i}$ are fuzzy sets described by membership functions $\mu_{A_{m,n}}(\nu_m) :\rightarrow [0,\ 1]$ and $\mu_{\bar{\Phi}_m} :\rightarrow [0,\ 1]$.

Then, an inference mechanism is used to calculate the degree to which each rule fires for a given fuzzified input pattern (ν_1, ν_2) by considering the label sets and rule.

In this work, the firing strength ω_n, the degree of firing for a rule, is calculated by the product of the degrees of membership, that is,

$$\omega_n = \prod_{m=1}^{2} \mu_{A_{m,n}}(\nu_m) \tag{29}$$

Finally, a defuzzifier converts the resulting fuzzy sets defined by the inference mechanism to a standard crisp signal. Here, we use the center-of-gravity or *centroid* method to calculate $\Phi_{i,i}(j)$ as follows:

$$\Phi_{i,i}(j) = \frac{\sum_{n=1}^{N_r} \omega_n \bar{\Phi}^n_{i,i}}{\sum_{n=1}^{N_r} \omega_n} \tag{30}$$

Comparing the iterative learning algorithm (27) and (28), we can see that (27) is equivalent to a traditional constant-gain PID controller, whereas (28) is equivalent to a varying-gain PID controller. Therefore, based on the performance of different PID controllers, we can state that if the coefficient matrix is carefully updated, the switching gain will take less time to reach an optimal value when using the iterative fuzzy logic update law.

B. Diagnostic Observer Using Second Order Sliding Mode

a nonlinear observer is proposed as follows:

$$\begin{aligned} \dot{\hat{x}}_1 &= \hat{x}_2 + z_1, \quad \hat{x}_1(0) = x_1 \\ \dot{\hat{x}}_2 &= f(t, \hat{x}_1, \hat{x}_2, u) + z_2 + \beta(t - T_m)\hat{M}_2(t),\ \hat{x}_2(0) = 0 \\ \hat{y} &= \hat{x}_1 \end{aligned} \tag{31}$$

where $\hat{x}_1$ and $\hat{x}_2$ are the estimated states, z_1 and z_2 are the correction variables, and $\hat{M}_2(t)$ is a vector of online estimators used to characterize the process faults. The term T_m is the beginning time that enables the wavelet networks. In order to investigate the properties of the sliding mode and the online estimators more clearly, we assume that $T_x < T_m < T_f$, where T_x is the time when state x_2 is observed by the second order sliding mode. Hence, the online fault estimation does not intervene with the state observation using the second order sliding mode.

The correction variables z_1 and z_2 are expressed as

$$\begin{cases} z_1 = \lambda_1 |\tilde{x}_1|^{1/2} \text{sign}(\tilde{x}_1) + v_1 \\ \dot{v}_1 = \alpha_1 \text{sign}(\tilde{x}_1) \end{cases} \tag{32}$$

and

$$\begin{cases} z_2 = 0 & \text{if } \dot{\tilde{x}}_1 \neq 0, \tilde{x}_1 \neq 0 \\ \quad = \lambda_2 |z_1|^{1/2} \text{sign}(z_1) + v_2 & \text{if } \dot{\tilde{x}}_1 = 0, \text{and } \tilde{x}_1 = 0 \\ \dot{v}_2 = \alpha_2 \text{sign}(z_1) \end{cases} \tag{33}$$

where $\tilde{x}_1 = x_1 - \hat{x}_1$ and $\tilde{x}_2 = x_2 - \hat{x}_2$ are denoted as the state estimation errors, and "sign" is the signum function.

Remark 2: In the above second-order sliding mode observer, anti-peaking structure is still used [19], [20], where $\tilde{x}_1$ and $\tilde{x}_2$ reach the sliding manifold one by one in a recursive way; that is, $\tilde{x}_1$ reaches the manifold before $\tilde{x}_2$.

C. Diagnostic Observer Using High Order Sliding Mode Differentiators

From system (18)-(21), the relative degree from the input, u, to the output, y, is more than one. When $f(x_1, x_2)$ and $h(x_1, x_2)$ are general nonlinear functions, the observer design for (18)-(21) becomes a challenging task if high order sliding mode techniques are not used.

Equations (20) and (21) indicate that the unmeasurable state x_2 can be represented as a nonlinear function of the system output and its derivative. Therefore, if we can obtain the derivatives of y, the state x_2 can be estimated using (20) and (21).

Second order or third order sliding mode differentiators [36] are used to obtain the first and second order derivatives of y, which are formulated as follows:

1) Second Order Sliding Mode Differentiator

$$\begin{aligned}\dot{z}_0 &= v_0\\ v_0 &= -\lambda_0|z_0 - y|^{2/3}sign(z_0 - y) + z_1\\ \dot{z}_1 &= v_1\\ v_1 &= -\lambda_1|z_1 - v_0|^{1/2}sign(z_1 - v_0) + z_2\\ \dot{z}_2 &= -\lambda_2 sign(z_2 - v_1).\end{aligned} \tag{34}$$

2) Third Order Sliding Mode Differentiator

$$\begin{aligned}\dot{z}_0 &= v_0\\ v_0 &= -\lambda_0|z_0 - y|^{3/4}sign(z_0 - y) + z_1\\ \dot{z}_1 &= v_1\\ v_1 &= -\lambda_1|z_1 - v_0|^{2/3}sign(z_1 - v_0) + z_2\\ \dot{z}_2 &= v_2\\ v_2 &= -\lambda_2|z_2 - v_1|^{1/2}sign(z_2 - v_1) + z_3\\ \dot{z}_3 &= -\lambda_3 sign(z_3 - v_2)\end{aligned} \tag{35}$$

where λ_0, λ_1, λ_2, and λ_3 are diagonal positive coefficient matrices.

The parameters of the differentiator can be easily adjusted because the estimation accuracy is not very sensitive to their values. However, a tradeoff exists: the larger the parameters, the faster the convergence and the higher sensitivity to input noises and the sampling interval.

It has been proved that if no measurement noise exists and all the coefficients are chosen properly, then, within a finite time, both the 2nd-order and 3rd-order sliding mode differentiators can guarantee

$$z_0 = y;\ z_1 = \dot{y};\ z_2 = \ddot{y}. \tag{36}$$

If measurement noise exists with a magnitude less than ϵ, and all the coefficients are chosen properly, the high order sliding mode differentiators can ensure

$$\begin{aligned}|z_i - y^{(i)}| &\le \mu_i \epsilon^{(n-i+1)/(n+1)},\ i = 0, 1, \cdots, n\\ |v_i - y^{(i+1)}| &\le \nu_i \epsilon^{(n-i)/(n+1)},\ i = 0, 1, \cdots, n-1\end{aligned} \tag{37}$$

where μ_i and ν_i are positive constants which are only dependent on the parameters of the differentiators [36].

A diagnostic observer using the second order or third order sliding mode differentiators is designed as follows,

$$\begin{aligned}\dot{\hat{x}}_2 &= f(y, \hat{x}_2) + Bu + \beta(t - T_m)\hat{M}_2(t)\\ x_{2D} &= h^{\dagger}(y, \dot{y}_D)\\ \hat{x}_2(0) &= x_{2D}(0)\end{aligned} \tag{38}$$

where $\hat{x}_2 \in \Re^n$ is the estimated state, $\dot{y}_D$ is the first-order derivative of y computed via the high order sliding mode differentiators, and x_{2D} is the calculated state using y and $\dot{y}_D$. If the high order sliding mode differentiators can exactly compute the derivative of y, then x_{2D} is completely equal to x_2. Moreover, we assume that the online fault estimator $\hat{M}_2(t)$ is activated after all the states are estimated via HOSMDs, but before the occurrence of any fault. This assumption guarantees the performance of the neural adaptive estimators.

V. Fault Diagnosis Schemes

In model-based fault diagnosis study, a residual is usually generated to detect and diagnose faults. Due to the universal existence of modeling uncertainties and disturbances, robust diagnosis strategies are necessary to avoid false alarm. One robust FD approach uses a dead-zone operator in the parameter update algorithm which hopes the estimator only to specify the signal with magnitude above a threshold. However, this method may affect the accuracy of fault estimation. Another way to realize robust fault detection is to set a nonzero threshold for the residual when making diagnostic decision.

In this work, the measurable output estimation error can be considered as the residual for robust fault detection. After the sliding mode term forces all the state estimation errors to reach the sliding manifold,

$$\begin{cases}\text{No fault has occured, } \hat{M}_1(t), \hat{M}_2(t) \text{ are set to zero}\\ \qquad \text{if } \|\tilde{y}(t)\| < \epsilon_f\\ \text{Fault has occurred, } \hat{M}_1(t), \hat{M}_2(t) \text{ are activated}\\ \qquad \text{if } \|\tilde{y}(t)\| \ge \epsilon_f\end{cases} \tag{39}$$

However, due to the compensation of the online estimators, $\|\tilde{y}(t)\|$ will return to zero shortly after the occurrence of a fault. In order to achieve fault isolation and estimation, we need to use the output signals of the estimators $\hat{M}_1(t)$ and $\hat{M}_2(t)$, which are designed to identify the location and magnitude of the fault.

VI. Online Fault Estimators

In the nonlinear diagnostic observer (22), online estimators $\hat{M}_1(t)$ and $\hat{M}_2(t)$ are used to characterize the fault. There exists a large number of online estimators, e.g., neural networks, fuzzy models and so on, which can approximate universal bounded nonlinear functions under certain conditions. However, considering the requirement of online real-time realization, the FD scheme should be able to be implemented as quickly as possible. As the algorithm becomes more complicated, the approximation performance may be better, however, the computation time probably increases as well. Hence, There is a trad-off between the simplification of FD scheme and the improvement of estimation performance.

In our recent studies, several online estimators were designed to achieve online fault estimation. These estimators can be classified into two classes, one is neural-based estimators and the other is iterative learning-based estimators.

A. Neural-based Estimators

1) Neural Adaptive Estimator: Instead of using a multi-layer feed-forward neural networks [7], we designed a neural adaptive estimator, which has the following structure [38]:

$$\hat{M}_{i,j}(t) = W_{i,j}(t)\sigma(V_{i,j}(t)I_{i,j}(t)) \tag{40}$$

where $\hat{M}_{i,j}(t), (i = 1, 2; j = 1, \cdots, p)$ is the (i,j)th element of $\hat{M}(t)$. $W_{i,j}(t)$ and $V_{i,j}(t) =$

$[V_{i,j}^{(1)}(t), \cdots, V_{i,j}^{(p+q)}(t)]^\top$ are the parameters of $\hat{M}_{i,j}(t)$ at time t, and $I_{i,j}(t) = [\hat{M}_{i,j}(t-\tau), \cdots, \hat{M}_{i,j}(t-p\tau), \tilde{x}_{i,j}(t-\tau), \cdots, \tilde{x}_{i,j}(t-q\tau)]^\top$, where τ here denotes the sampling time interval, $\tilde{x}_{i,j}$ is the (i,j)th state estimation error which is obtained via the sliding mode observer. The term $\sigma(x) = (1-\mathrm{e}^{-x})/(1+\mathrm{e}^{-x})$ is a hyperbolic tangent activation function.

The estimator is recursively updated by previous p step estimator outputs and previous q step state estimation errors. The choice of tapped delay p and q is based on a heuristic or called trial-and-error method. Although using large p and q probably guarantees convergence and increases approximation accuracy, it may spend more computation time and cause unnecessary time delay.

2) Neural State Space Model-based Estimator: Neural state space (NSS) model is a special kind of recurrent neural networks, which not only has the same universal approximation ability as neural networks, but also has a similar structure with linear state space model. This feature makes the theoretical analysis of NSS model-based system more conveniently.

The dynamics of the neural state space model-based estimator is [39]

$$\dot{\hat{M}}_{i,j}(t) = W_{i,j}^{(1)}(t)\hat{M}_{i,j}(t) + W_{i,j}^{(2)}(t)\sigma\big(W_{i,j}^{(3)}(t)\hat{M}_{i,j}(t) + W_{i,j}^{(4)}(t)\tilde{x}_{i,j}(t)\big) \quad (i = 1, \cdots, p) \tag{41}$$

where $W_{i,j}^{(l)}(i = 1, 2; j = 1, \cdots, p; l = 1, \cdots, 4)$ are the parameters of the NSS model.

3) Wavelet Networks: Some studies have proved that in some cases, a simple-structure wavelet network can at least provide the same approximation ability as traditional neural networks [40]. This feature implies wavelet network can also be used as the estimator.

We proposed a three-layer wavelet network that is composed of an input layer (the i layer), a wavelet layer (the ij layer), and an output layer (the o layer) [41]. The schematic of this wavelet network is shown in Fig. 2. The inputs of the wavelet network are the state estimation errors obtained from the sliding mode observer and the difference between the network input and output. The output of the wavelet network is the estimation of the fault.

The input-output relation for node i of the input layer is

$$\mathrm{net}_i^1 = ni_i, \quad no_i^1 = f_i^1(\mathrm{net}_i^1) = \mathrm{net}_i^1, \quad i = 1, \cdots, p \tag{42}$$

where ni_i is the input of the wavelet network in which $ni_1 = \tilde{x}_{i,j}$, and $ni_2 = ni_1 - \hat{M}_{i,j}$. Moreover, in the wavelet layer, a family of wavelets is established by preforming translations and dilations on a single fixed function called the mother wavelet. In this study, the first derivative of a Gaussian function $\phi(x) = -x\exp(-x^2/2)$ is selected as the mother wavelet. This mother wavelet function has a universal approximation ability, since it can be regarded as a differentiable version of the Haar mother wavelet, just as the sigmoid is a differentiable version of a step function. For the ijth node in the wavelet layer, we have

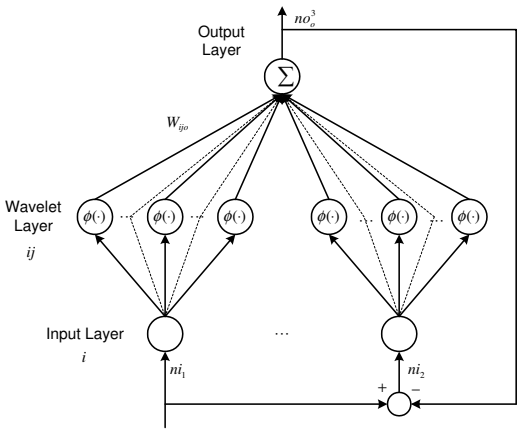

Figure 2. Structure of the three-layer wavelet network

$$\mathrm{net}_{ij}^2 = \frac{no_i^1 - c_{i,j}}{\sigma_{ij}} \tag{43}$$

$$no_{ij}^2 = \phi_{ij}(\mathrm{net}_{ij}^2) = -\mathrm{net}_{ij}^2 \exp\big(-(\mathrm{net}_{ij}^2)^2/2\big), j = 1, \cdots, q \tag{44}$$

where c_{ij} and σ_{ij} are the translation and dilation in the jth term of the ith input no_i^1 to the node of mother wavelet layer, respectively, and q is the total number of the wavelets with respect to the corresponding input node.

In the output layer, the single node o is labeled as $\sum$, which adds all input signals together.

$$\mathrm{net}_o^3 = \sum_{ij} W_{ijo}^3 no_{ij}^2 \tag{45}$$

$$no_o^3 = f_o^3(\mathrm{net}_o^3) = \mathrm{net}_o^3, \quad o = 1 \tag{46}$$

where $no_o^3 = \hat{M}_{i,j}$ is the output of the wavelet network; the connection weight W_{ijo}^3 is the output action strength of the oth output associated with the ijth wavelet, and no_{ij}^2 is denoted as the ijth input to the node of output layer.

B. Fault Estimators Using Iterative Learning Algorithms

Although neural-based estimators can approximate the fault with high accuracy in a short time, there inevitably exists overshoot and transient process in the fault estimation, because the estimator needs time to update its parameters to track an abrupt change. Accordingly, we proposed several kinds of iterative learning estimators, which have the following characteristics: i) The tracking trajectory becomes time-varying but iteration-invariant. ii) The parameters of the estimator are updated in the iteration domain rather than in the time domain. ii) When the convergence of the update process in iteration domain is guaranteed, the overshoot and transient process in fault estimation are eliminated.

1) PID-type Iterative Learning Estimator: Inspired by the structure of the single neuron PID controller [42], the proposed PID-type iterative learning estimator is described as,

$$M_{i,j}(t) = \frac{K \cdot \sum_{l=1}^{3} \omega_{i,j}^{(l)}(t) z_{i,j}^{(l)}(t-\tau)}{\sum_{l=1}^{3} \omega_{i,j}^{(l)}(t)} \tag{47}$$

where K is the learning coefficient, $\omega_{i,j}^{(l)}(t), (i = 1,2,; j = 1,\cdots,p; l = 1,\cdots,3)$ are the three parameters of the (i,j)th $\hat{M}(t)$, and τ is the sampling time interval in the iteration domain. Three exogenous inputs are chosen as

$$\begin{cases} z_{i,j}^{(1)}(t) = \tilde{x}_{i,j}(t) \\ z_{i,j}^{(2)}(t) = z_{i,j}^{(1)}(t) - M_{i,j}(t) \\ z_{i,j}^{(3)}(t) = \Delta z_{i,j}^{(2)}(t) = z_{i,j}^{(2)}(t) - z_{i,j}^{(2)}(t-\tau) \end{cases} \tag{48}$$

Since this estimator is a linear network, some adaptive algorithms can be used to update its parameters [43].

2) Iterative Neuron PID Estimator: The above PID-type iterative learning estimator is actually a linear combination of previous information of state estimation error and fault estimation error. In order to accelerate the convergence speed, the nonlinear activation function is used and formulate an iterative neuron PID estimator in [44] as,

$$\begin{aligned} \hat{M}_{i,j}(t) = \hat{M}_{i,j}(t-\tau) + W_{i,j}(t)\sigma\Big(V_{i,j}^{(1)}(t) z_{i,j}^{(1)}(t) \\ + V_{i,j}^{(2)}(t) z_{i,j}^{(2)}(t) + V_{i,j}^{(3)}(t) z_{i,j}^{(3)}(t)\Big) \end{aligned} \tag{49}$$

where $\hat{M}_{i,j}(t)$ is the (i,j)th element of $\hat{M}(t)$. $W_{i,j}$ and $V_{i,j}^{(l)}$, $(l = 1,2,3)$ are the parameters of the estimator. The term $\sigma(\cdot)$ is still the hyperbolic tangent activation function. Defining $e_{i,j}(t) = \tilde{x}_{i,j}(t) - \hat{M}_{i,j}(t)$, the exogenous inputs of $\hat{M}_{i,j}(t)$ are chosen as

$$\begin{cases} z_{i,j}^{(1)}(t) = e_{i,j}(t) \\ z_{i,j}^{(2)}(t) = \Delta e_{i,j}(t) = e_{i,j}(t) - e_{i,j}(t-\tau) \\ z_{i,j}^{(3)}(t) = \Delta^2 e_{i,j}(t) \\ \qquad = e_{i,j}(t) - 2e_{i,j}(t-\tau) + e_{i,j}(t-2\tau) \end{cases}$$

For the parameter update of this estimator, four robust parameter update laws were proposed in [44]. In addition to the traditional parameter update law for neural networks, like gradient descent algorithm and extended Kalman filtering algorithm, two iterative learning algorithms were designed, which use the fault estimation error at current and previous iterations.

C. Parameter Update Law

For above online fault estimators, in order to characterize the fault as soon as possible, the parameters are supposed to be updated using some optimization algorithms. The parameter update algorithms for recurrent neural networks are all suitable for above estimators, for example, dynamic back-propagation method, extended Kalman filtering algorithm, etc. Moreover, two robust iterative learning algorithms were designed to update the parameters in the iterative neuron PID estimators [44].

VII. Conclusion

In this paper, we summarized our research work on robust fault diagnosis for satellite control systems using sliding mode and learning approaches in recent years. Firstly, mathematical models for a variety of satellite control systems were summarized and analyzed. These satellite control systems can be classified into two classes of nonlinear dynamics, which were used to design different robust fault diagnosis schemes. In our proposed robust FD schemes, sliding mode observer was integrated with online learning estimators for the purpose of fault detection, isolation, and estimation. The sliding mode observer with time-varying switching gain estimate the states as soon as possible before the occurrence of any fault. Then, the online learning estimators were used to identify the fault from the state estimation error with sufficient accuracy. In order to simplify the FD algorithm under the guarantee of fault estimation performance, some neural-based estimators and iterative learning estimators were designed.

In practical applications, single FD scheme for a satellite system might be not able to reach the same performance as that in simulation due to the complex situation in space. Hence, using multiple FD algorithms in a distribute and simultaneous way, we can achieve software redundancy to reduce fault false alarm.

Moreover, in our above research, state observers were designed only for a specific class of nonlinear systems, which can not describe a few classes of satellites. Therefore, for general nonlinear satellite systems, we need to design other state observers for the purpose of fault detection, isolation and estimation.

Acknowledgment

This research was supported by Natural Sciences and Engineering Research Council (NSERC) of Canada and the Canadian Space Agency (CSA) under a joint multi-university project entitled Intelligent Autonomous Space Vehicles (IASV): Health monitoring, fault diagnosis and recovery.

References

[1] R.J. Patton, P.M. Frank and R.N. Clark, *Fault Diagnosis in Dynamic Systems: Theory and Applications*, Prentice-Hall, Englewood Cliffs, NJ; 1989.

[2] J.J. Gertler, *Fault Detection and Diagnosis in Engineering Systems*, Marcel Dekker, NY; 1998.

[3] J. Chen and R.J. Patton *Robust Model-Based Fault Diagnosis for Dynamic Systems*, Kluwer Academic Publishers, Boston; 1999.

[4] R.J. Patton, R. Clark, and R.N. Clark, *Issues of Fault Diagnosis for Dynamic Systems*, Springer-Verlag, London; 2000.

[5] S. Naidu, E. Zafirou, and T.J. Mcavoy, "Use of Neural-Networks for Failure Detection in A Control System," *IEEE Control Syst. Mag.*, vol. 10, 1990, pp. 49-55.

[6] T. Marcu, and L. Mirea, "Robust Detection and Isolation of Process Faults Using Neural Networks," *IEEE Control Syst. Mag.* vol. 17, 1997, pp. 72-79.

[7] A.B. Trunov, and M.M. Polycarpou, "Automated Fault Diagnosis in Nonlinear Multivariable Systems Using A Learning Methodology," *IEEE Trans. Neural Networks*, vol. 11, 2000, pp. 91-101.

[8] W. Chen, and M. Saif, 2006, "An Iterative Learning Observer for Fault Detection and Accommodation in Nonlinear Time-Delay Systems," *Int. J. Robust and Nonlinear Contr.*, vol. 16, 2006, pp. 1-19.

[9] B. Jiang, and M. Staroswiecki, 2002, "Adaptive Observer Design for Robust Fault Estimation," *Int. J. Syst. Sci.*, vol. 33, 2002, pp. 767-775.

[10] A. Alessandri, "Fault Diagnosis for Nonlinear Systems Using A Bank of Neural Estimators," *Computers in Industry*, vol. 52, 2003, pp. 271-289.

[11] A. Xu, and Q. Zhang, "Nonlinear System Fault Diagnosis based on Adaptive Estimation," *Automatica*, vol. 40, 2004, pp. 1181-1193.

[12] M.M. Polycarpou, and A.J. Helmicki, "Automated Fault Detection and Accommodation: A Learning Systems Approach," *IEEE Trans. Syst., Man, and Cybern.*, vol. 25, 1995, pp. 1447-1458.

[13] A.T. Vemuri, and M.M. Polycarpou, "Robust Nonlinear Fault Diagnosis in Input-output Systems," *Int. J. Contr.*, vol. 68, 1997, pp. 343-360.

[14] M.A. Demetriou, and M.M. Polycarpou, "Incipient Fault Diagnosis of Dynamical Systems Using Online Approximators," *IEEE Trans. Automat. Contr.*, vol. 43, 1998, pp. 1612-1617.

[15] C. Edwards, and S.K. Spurgeon, "On the Development of Discontinuous Observers," *Int. J. Contr.*, vol. 59, 1994, pp. 1211-1229.

[16] S. Drakunov, and V. Utkin, "Sliding Mode Observers. Tutorial," In *Proeedings of the 34th Conference on Decision and Control*, Dec. 1995; New Orleans, LA, USA. pp. 3376-3378.

[17] I. Haskara, U. Ozguner, and V. Utkin, "On Sliding Mode Observers via Equivalent Control Approach," *Int. J. Contr.*, vol. 71, 1998, pp. 1051-1067.

[18] F. Floret-Ponetet, and F. Lamnabhi-Lagarrigue, "Parametric Identification Methodology Using Sliding Modes Observer," *Int. J. Contr.*, vol. 74, 2001, pp. 1743-1753.

[19] J.P. Barbot, and T. Boukhobza and M. Djemai, "Sliding Mode Observer for Triangular Input Form," *Proceedings of the 35th Conference on Decision and Control*, 1996, pp. 1489-1490.

[20] Y. Xiong, and M. Saif. "Sliding Mode Observer for Nonlinear Uncertain Systems," *IEEE Trans. Automat. Contr.*, vol. 46, 2001, pp. 2012-2017.

[21] T. Boukhobza, and J.P. Barbot, "High Order Sliding Modes Observer," In *Proceedings of the 37th IEEE Conference on Decision and Control* Dec. 1998; Tampa Florida, USA. pp. 1912-1917.

[22] J. Davila, L. Fridman, and A. Levant, "Second-order Sliding Mode Observer for Mechanical Systems," *IEEE Trans. on Automat. Contr.*, vol. 50, 2005, pp. 1785-1789.

[23] C. Edwards, S.K. Spurgeon, and R.J. Patton, "Sliding Mode Obsevers for Fault Detection and Isolation," *Automatica*, vol. 36, 2000, pp. 541-553.

[24] C.P. Tan, and C. Edwards, "Sliding Mode Observers for Detection and Reconstruction of Sensor Faults," *Automatica*, vol. 38, 2002, pp. 1815-1821.

[25] W. Chen, and M. Saif, "Robust Fault Detction and Isolation in Constrained Nonlinear Systems via A Second Order Sliding Mode Observer," In *Proc. of the 15th Triennial World Congress of IFAC*, Barcelona Spain, July 2002.

[26] T. Floquet, J.P. Barbot, et al, "On the Robust Fault Detection via A Sliding Mode Disturbance Observer," *Int. J. Contr.*, vol. 77, 2004, pp. 622-629.

[27] C. Edwards, and L. Fridman, and M-W.L. Thein, "Fault Reconstruction in a Leader/Follower Spacecraft System Using Higher Order Sliding Mode Observers," *Proceedings of the American Control Conference*, New York, July 2007, pp. 408-413.

[28] Q. Wu and M. Saif, "Robust Fault Diagnosis for a Satellite System Using a Neural Sliding Mode Observer," *in Proc. of the 44th IEEE Conference on Decision and Control, and European Control Conference ECC 2005 (CDC-ECC'05)*, Seville, Spain, December 12-15, 2005, pp. 7668-7673.

[29] A.A. Anchev, "Equilibrium Attitude Transitions of a Three Rotor Gyrostat in a Circular orbit," *Journal of the American Institute of Aeronautics and Astronautics*, vol. 11, 1973, pp. 467-472.

[30] C.D. Yang, and Y.P. Sun, Mixed H_2/H_∞ Sate-feedback Design for Micorsatellite Attitude Control, *Control Engineering Practice*, vol. 10, 2002, pp. 951-970.

[31] B. Wie, *Space Vehicle Dynamics and Control*, American Institute of Aeronautics and Astronautics Inc., Reston, 1998.

[32] S.N. Singh and R. Zhang, "Adaptive Output Feedback Control of Spacecraft with Flexible Appendages by Modeling Error Compensation," *Acta Astronautica*, vol. 54, 2004, pp. 229-243.

[33] K. Karray, A. Grewal, et al, "Stiffening Control of a Class of Nonlinear Affine Systems," *IEEE Trans. Aerosp. Electron. Syst.*, vol. 33, 1997, pp. 473-484.

[34] R. Marino, and P. Tomei, *Nonlinear Control Design, Geometric, Adaptive and Robust*, Prentice Hall, UK, 1995.

[35] W.E. Dixon, A.Behal et al, *Nonlinear Control of Engineering Systems–A Lyapunov-Based Approach*, Birkhauser, 2003.

[36] A. Levant, "Robust Exact Differentiation via Sliding Mode Technique", *Automatica*, vol. 34, No. 3, 1998, pp. 379-384.

[37] Q. Wu, and M. Saif, "Robust Fault Detection and Diagnosis in a Class of Nonlinear Systems Using a Neural Sliding Mode Observer," *Accepted by the International Journal of Systems Science-Special Issue on Advances in Sliding Mode Observation and Estimation*, 207.

[38] Q. Wu and M. Saif, "Neural Adaptive Observer Based Fault Detection and Identification for Satellite Attitude Control Systems," *in Proc. of the 2005 American Control Conference*, June 8-10, Portland, Oregon, USA, 2005, pp. 1054-1059.

[39] Q. Wu and M. Saif, "Robust Fault Diagnosis for Satellite Attitude Systems Using Neural State Space Models," *in Proc. of the International Conference on Systems Man and Cybernetics*, Hawaii, USA, October 10-12, 2005, pp. 1955-1960.

[40] Q. Zhang, and A. Benveniste, "Wavelet Networks," *IEEE Trans. Neural Networks*, vol. 3, 1992, pp. 889-898.

[41] Q. Wu and M. Saif, "Robust Fault Detection and Diagnosis for a Multiple Satellite Formation Flying System Using Second Order Sliding Mode and Wavelet Networks," *Accepted by the 2007 American Control Conference*, New York, USA, July 11-13, 2007.

[42] Z. Li, R. Zhao Y. Li and D. Sun, "Real-Time Predictable Control Based on Single-Neuron PSD Controller," *in Proc. of the Second Internatioal Conference on Machine Learning and Cybernetics*, Xi'an, Nov., 2003, pp. 720-725.

[43] Q. Wu and M. Saif, "Observer-Based Robust Process Fault Detection and Diagnosis for a Satellite System with Flexible Appendages," *in Proc. of the 45th Conference on Decision and Control*, San Diego, CA, USA, Dec. 13-15, 2006, pp. 2183-2188.

[44] Q. Wu and M. Saif, "Robust Fault Diagnosis for a Satellite Large Angle Attitude System Using an Iterative Neuron PID (INPID) Observer," *in Proc. of the 2006 American Control Conference*, Minneapolis, Minnesota USA, June 14-16, 2006, pp. 5710-5715.

Qing Wu is currently an embedded software engineer at Critical Environment Technologies Canada Inc., Delta, BC, Canada. He received his PhD degree in Engineering Science from Simon Fraser University, Vancouver, BC, Canada in 2008, MS and BS degrees in Control Theory and Engineering from Huazhong University of Science and Technology, Wuhan, China in 1999 and 2002, respectively. His research interests include fault diagnosis, computational intelligence, control systems, sensors, etc.

Mehrdad Saif received B.S. in 1982, M.S. in 1984, and PhD in 1987 all in Electrical Engineering. During his graduate studies he worked on research projects sponsored by NASA Lewis (now Glenn) Research Center, as well as Cleveland Advanced Manufacturing Program (CAMP). In 1987 he joined the School of Engineering Science at Simon Fraser University as an Assistant Professor. He is currently a Full Professor and Director of the same School. From 1993-1994 Saif was a Visiting Scholar at General Motors North American Operation (NAO) R & D Center in Warren, MI. At GM he was a member of the Powertrain Control Group in the Electrical and Electronics Research Department where he worked on engine control and on-board engine diagnostic problems.

Saif's research interests are in estimation and observer theory, model based fault diagnostics, and application of these to automotive, power, and other complex engineering systems. He has published over 150 refereed journal and conference papers plus an edited book in these areas. Saif has been a consultant to a number of industries and agencies such as GM, NASA, B.C. Hydro, Ontario Council of Graduate Studies, etc. He served two terms (1995,1997) as the Chairman of the Vancouver Section of the IEEE Control Systems Society, and is currently a member of the editorial board of the IEEE Systems Journal, International Journal of Control and Computers, IEEE CDC, and ACC. Saif is Senior Member of IEEE and a Registered Professional Engineer in British Columbia.